Scientific Research Publishing

Journal of Applied Mathematics and Physics, 2025, 13(5), 1665-1682
https://www.scirp.org/journal/jamp
ISSN Online: 2327-4379
ISSN Print: 2327-4352

Improved Two-Stage Epidemic Dynamics Model

Shijun Gao[1], Xinzhe Yao[2], Hua He[1*]

[1]School of Science, Hebei University of Technology, Tianjin, China
[2]School of Statistics and Data Science, Nankai University, Tianjin, China
Email: 2021433@hebut.edu.cn, 2120230137@mail.nankai.edu.cn, *hehua@hebut.edu.cn

How to cite this paper: Gao, S.J., Yao, X.Z. and He, H. (2025) Improved Two-Stage Epidemic Dynamics Model. *Journal of Applied Mathematics and Physics*, **13**, 1665-1682.
https://doi.org/10.4236/jamp.2025.135092

Received: April 7, 2025
Accepted: May 9, 2025
Published: May 12, 2025

Abstract

Infectious diseases have always been critical factors affecting human life, health, and social stability throughout history. The recurrent epidemics of infectious diseases have caused enormous disasters for human survival and national well-being. Establishing mathematical models to describe the transmission process of infectious diseases, analyze the variation patterns of infected individuals, and predict disease outbreak timing is significant for providing a decision-making basis to prevent the spread of infectious diseases. The use of dynamic models specific to infectious diseases offers unique advantages in addressing these issues. In this paper, a two-stage infectious disease dynamics model with a latent period and asymptomatic infection is established to model the transmission of highly infectious pathogens in a population. Utilizing epidemic data from Shanghai spanning February 8, 2022, to July 1, 2022, the model is numerically simulated, and the basic reproduction number R_0 for the two stages is calculated using the next generation matrix method. Studies indicate that timely enhancements in epidemic control measures can significantly reduce the number of confirmed cases in hospitals, decrease the peak number of infections, and hasten the arrival of the epidemic's inflection point.

Keywords

Epidemic Dynamics Model, Numerical Simulation

1. Introduction

In the past 30 years, research on infectious disease dynamics has advanced rapidly worldwide, with numerous mathematical models being employed to analyze various infectious disease issues. Mathematical modeling has proven to be an invaluable tool for understanding the mechanisms of infectious disease transmission, assessing intervention strategies, and predicting outbreak trajectories [1]-[3].

These models provide critical insights that help public health authorities make informed decisions to mitigate the spread of infectious diseases. Importantly, mathematical models not only facilitate the identification of key parameters that influence the course of an epidemic but also allow for the evaluation of potential intervention strategies before they are implemented in real-world settings [4].

Most of these models rely on systems of ordinary differential equations (ODEs) to describe the evolution of disease states within a population. Such models typically include compartments representing different health states, such as susceptible, infected, recovered, or vaccinated individuals. The Susceptible, Exposed, Infectious, Recovered (SEIR) model is one of the most commonly employed frameworks in this field, given its ability to account for the incubation period of an infectious disease. In the context of COVID-19, SEIR-based models have been widely used to predict epidemic trajectories, assess public health interventions, and estimate the basic reproduction number (often denoted as R_0).

Mwalili *et al.* utilized an enhanced SEIR model to evaluate epidemiological dynamics under various intervention strategies, such as social distancing and quarantines, aimed at mitigating the spread of COVID-19 [3]. Using the next-generation matrix method, they calculated the basic reproductive number (R_0), demonstrating that strategic isolation of patients and close contacts could effectively reduce transmission. Meanwhile, Wu employed the SEIR model to incorporate factors such as the source of infection and human mobility during the Spring Festival in Wuhan, thereby estimating the dynamics of the outbreak in Wuhan [4].

Moreover, Din R U *et al.* used a SIR model with a convex incidence for a mathematical analysis of COVID-19 [5]. Liu *et al.* examined the dynamics of SIR epidemiological models with changing population sizes and switching regimes [6]. Alenezi M N *et al.* developed a reasonable SIR estimation model for the spread of COVID-19 in Kuwait [7]. De La Sen M *et al.* studied a discrete SEIR model with two doses of delayed feedback vaccine control on susceptible individuals [8]. Kundu S *et al.* investigated a multi-delay SEIR model with an immune phase and therapeutic function [9]. Li Y *et al.* studied a class of diffusion SEIR models with a general incidence [10]. Youssef H *et al.* studied the SEIQR model and applied it to the COVID-19 epidemic in Saudi Arabia [11].

While these models have made substantial contributions to understanding disease transmission, they often operate under assumptions that may not be entirely representative of real-world conditions. For instance, most modeling analyses assume that prevention and control measures are static and that recovered individuals are immune to reinfection. However, such assumptions may be unrealistic when considering the evolving nature of pathogen virulence, public health policies, and behavioral responses to pandemics. The rapid mutation rate of pathogens like SARS-CoV-2, along with the inconsistent application of control measures and the possibility of reinfection, challenge the applicability of traditional compartmental

models [12]. Therefore, a more flexible and realistic approach is needed to represent the temporal dynamics of disease transmission [13]-[25].

To address these limitations, our study presents a novel two-stage SEIAHDR_Q model (Susceptible, Exposed, Infected, Asymptomatic, Hospitalized, Dead, Recovered, Quarantined) that builds upon existing compartmental models to incorporate the complexities of real-world epidemic spread. The proposed model introduces time-varying parameters for the infection rate, recovery rate, and diagnosis rate, which allows it to capture dynamic changes in disease transmission due to factors such as government interventions, public behavior modifications, and changes in pathogen characteristics. The model is divided into two distinct stages: the first stage includes the implementation of isolation measures following epidemiological investigations, while the second stage introduces time-dependent parameters to better reflect ongoing changes in control measures and transmission dynamics.

2. Two-Stage SEIAHDR_Q Model

Considering the distinct transmission characteristics of highly infectious pathogenic microorganisms, we have devised a bifurcated infectious disease dynamics model to represent their spread. This model integrates governmental prevention strategies, such as quarantining key epidemic areas, conducting epidemiological investigations, suspending non-essential production and lifestyle activities, and establishing makeshift hospitals, as well as various categories of infected individuals.

The model is based on the following assumptions, derived from the transmission characteristics of highly infectious pathogenic microorganisms:

1) Despite significant population movement, different individual types are uniformly distributed.

2) A small minority of individuals have innate immunity, rendering the majority susceptible.

3) After infection with such pathogens, the human body undergoes an incubation period, during which the infected person remains infectious.

4) Most infected individuals exhibit asymptomatic infection throughout the infection phase and are still contagious [26].

5) Once all infected individuals are hospitalized, their ability to infect others is eliminated.

6) The population that has recovered and been discharged can potentially experience secondary infection.

2.1. Phase I: The Low-Intensity Control Period (February 22, 2022-April 15, 2022)

During this period, the model encompasses eight demographic states: Susceptible (S), Exposed (E), Infectious (I), Asymptomatic Infectious (I_A), Hospitalized (H), Deceased (D), Recovered (R), and Quarantined Exposed (Q_E). For sim-

plicity, $S(t)$, $E(t)$, and so on are considered as the corresponding population numbers at time t. The specific transmission mechanism is detailed as follows:

Infection process: All virus carriers (states E, I, and I_A) possess the potential to infect a susceptible host at any given moment t, progressing it to the subsequent state.

Isolation measures: Certain individuals in state E will be quarantined based on epidemiological investigation findings (close contacts and sub-close contacts), transitioning to the state. Some individuals in the state who test positive for nucleic acid will progress to the or H state, contingent on symptom presence, while others will be discharged from quarantine and revert to state S.

Diagnosis process: After the incubation period, some individuals in states I and will manifest symptoms and be admitted for treatment (state H), during which they will cease to infect other susceptible individuals.

Figure 1 provides a depiction of the model's flow chart.

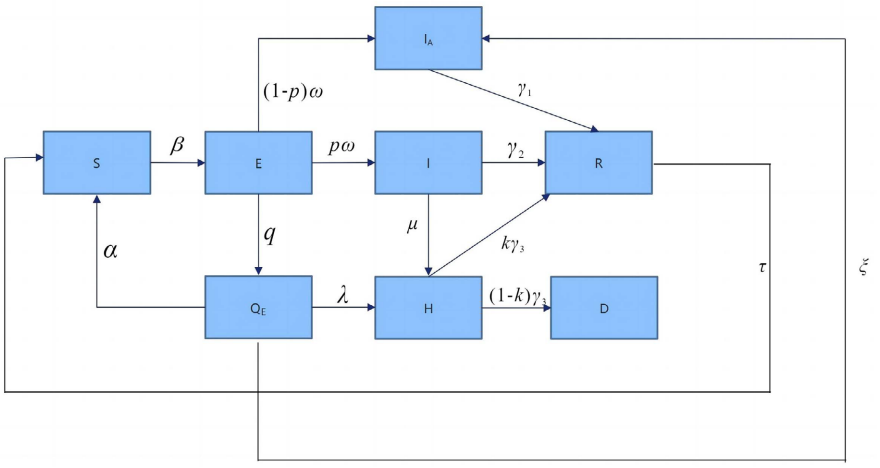

Figure 1. The compartment diagram of infectious disease dynamics model in low-intensity control period.

Recovery and death process: Individuals in states I_A, I, and H will recover to form state R at a certain rate and proportion. A specific percentage of state R individuals will become susceptible to re-infection within a brief period. State H individuals will succumb to the virus according to a predetermined proportion and rate.

The example flowchart is illustrated in Figure 1.

We derived a dynamic model described by the following differential equations:

$$\frac{\mathrm{d}S(t)}{\mathrm{d}t} = -c_2\beta\frac{S(t)}{N}\left(\sigma E(t)+\eta I_A(t)+I(t)\right)+\tau R(t)+\alpha Q_E(t) \tag{1}$$

$$\frac{\mathrm{d}E(t)}{\mathrm{d}t} = (1-q_0)c_2\beta\frac{S(t)}{N}\left(\sigma E(t)+\eta I_A(t)+I(t)\right)-\omega E(t) \tag{2}$$

$$\frac{\mathrm{d}I_A(t)}{\mathrm{d}t} = (1-p)\omega E(t)-\gamma_1 I_A(t)+\xi Q_E(t) \tag{3}$$

$$\frac{\mathrm{d}I(t)}{\mathrm{d}t} = p\omega E(t) - (\gamma_2 + \mu_2) I(t) \tag{4}$$

$$\frac{\mathrm{d}Q_E(t)}{\mathrm{d}t} = q_0 c_2 \beta \frac{S(t)}{N} \left(\sigma E(t) + \eta I_A(t) + I(t)\right) - (\lambda + \alpha + \xi) Q_E(t) \tag{5}$$

$$\frac{\mathrm{d}H(t)}{\mathrm{d}t} = \lambda Q_E(t) + \mu_2 I(t) - \gamma_3 H(t) \tag{6}$$

$$\frac{\mathrm{d}R(t)}{\mathrm{d}t} = \gamma_1 I_A(t) + \gamma_2 I(t) + \kappa_0 \gamma_3 H(t) - \tau R(t) \tag{7}$$

$$\frac{\mathrm{d}D(t)}{\mathrm{d}t} = (1 - \kappa_0) \gamma_3 H(t) \tag{8}$$

2.2. Parameter Assignment and Estimation during the Low-Intensity Control Period

Relevant literature was consulted to provide the parameters c_2, σ, η, p, ω, γ_1, γ_2, γ_3 and λ as well as the initial values N, $I_A(t_0)$, $Q_E(t_0)$, $H(t_0)$, $D(t_0)$, $R(t_0)$ and $D(t_0)$ for the disease. The initial stage model comprises seven unknown parameters: β, τ, α, q_0, κ_0, ξ, and μ_2. Many parameters within the model require fitting. Based on the epidemic data from Shanghai between February 22, 2022, and April 15, 2022 (refer to the **Appendix**), a genetic algorithm was utilized to fit these unknown parameters. Table 1 presents the fitting results and comprehensive definitions of each parameter.

Table 1. Phase I model parameter assignment and significance.

Parameter	Definitions	Estimated Mean Value
c_2	Daily contact rate of infected people in the first stage	10 [27]
σ	Latent infection rate attenuation factor	0.50
η	Latent infection rate attenuation factor	0.70 [28]
p	Proportion of dominant infection	0.40
ω	The rate of latency to onset	1/5.2 [29]
γ_1	Recovery rate of asymptomatic patients	1/6 [30]
γ_2	Recovery rate of patients	1/8 [31]
γ_3	Recovery rate of diagnosed patients	1/10
λ	Diagnosis rate of isolated close contacts	1/7 [31]
β	Initial infection probability	0.05
τ	Secondary infection rate	0.60
α	The proportion of uninfected people after isolation as close contacts	0.16
q_0	Initial isolation ratio	0.21
k_0	The proportion of recovery of confirmed patients under initial conditions	0.99
ξ	Proportion of asymptomatic infection after isolation as close contacts	0.76
μ_2	The fastest diagnosis rate	0.20

2.3. Phase II: High-Intensity Control Period (April 16, 2022-July 1, 2022)

With the implementation of government epidemic prevention measures, an increase in the number of individuals in isolation and hospitalization was noted. Concurrently, the daily contact rate of infected individuals has been observed to decrease over time. There is an expected rise in the confirmation rate of hospitalized patients and the isolation rate of individuals who have had close contact with infected patients. The exponential function is used to model the dynamic patterns of $c(t)$, $\mu(t)$, and $q(t)$, with the respective functional representation provided as follows [32]:

$$c_t = c_0 \mathrm{e}^{-\alpha_1(i-1)} \tag{9}$$

$$q_t = (q_0 - q_m)\mathrm{e}^{-\alpha_2(i-1)} \tag{10}$$

$$\mu_t = (\mu_1 - \mu_m)\mathrm{e}^{-\alpha_3(i-1)} \tag{11}$$

The recovery rate of diagnosed patients has been observed to adhere to a sigmoid growth curve. To emulate this trend, we employed the growth curve to establish a fitting function for the recovery rate. The resultant function is expressed as follows [32]:

$$\kappa_t = \frac{\kappa_m}{1 + a\mathrm{e}^{-b(i-1)}} \tag{12}$$

The model incorporates a "Q_S" compartment to represent the dynamic process of enhancing isolation protocols for individuals suspected of infection.

The high-intensity management period is characterized by nine distinct states: S, E, I, I_A, H, D, R, Q_E, Q_S. To maintain brevity, we denote the state variables at time t as $S(t)$, $E(t)$ and so forth. It is noteworthy that the virus transmission process in the subsequent stage differs from the initial stage in the following manner:

The infection process: As epidemic prevention and control measures are implemented, the daily contact rate of individuals in states E, I and I_A with susceptible individuals, denoted by $c(t)$, decreases over time.

Isolation measures: Initiated by the Q_S compartment, the isolation rate of individuals who have had close contact with confirmed cases is expected to increase progressively.

Diagnostic process: With the support of medical teams from other regions, the confirmation rate of patients is anticipated to rise gradually.

Recovery and death process: The recovery and mortality process follows the sigmoid growth curve, influencing the recovery rate of patients.

Figure 2 provides a depiction of the model's flow chart.

A dynamic model was derived using the following set of differential equations:

$$\begin{aligned}\frac{\mathrm{d}S(t)}{\mathrm{d}t} = &-\left(\beta + q_t(1-\beta)\right)c_t \frac{S(t)}{N}\left(\sigma E(t) + \eta I_A(t) + I(t)\right) \\ &+ \delta Q_S(t) + \tau R(t) + \alpha Q_E(t)\end{aligned} \tag{13}$$

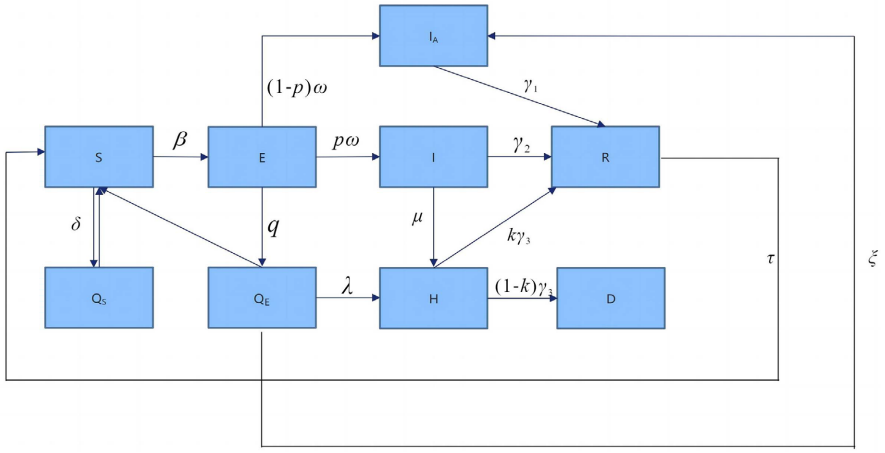

Figure 2. Infectious disease dynamics model compartment diagram of high intensity control period.

$$\frac{\mathrm{d}E(t)}{\mathrm{d}t}=(1-q_t)c_t\beta\frac{S(t)}{N}\left(\sigma E(t)+\eta I_A(t)+I(t)\right)-\omega E(t) \tag{14}$$

$$\frac{\mathrm{d}I_A(t)}{\mathrm{d}t}=(1-p)\omega E(t)-\gamma_1 I_A(t)+\xi Q_E(t) \tag{15}$$

$$\frac{\mathrm{d}I(t)}{\mathrm{d}t}=p\omega E(t)-(\gamma_2+\mu_t)I(t) \tag{16}$$

$$\frac{\mathrm{d}Q_S(t)}{\mathrm{d}t}=q_t(1-\beta)c_t\frac{S(t)}{N}\left(\sigma E(t)+\eta I_A(t)+I(t)\right)-\delta Q_S(t) \tag{17}$$

$$\frac{\mathrm{d}Q_E(t)}{\mathrm{d}t}=q_t c_t\beta\frac{S(t)}{N}\left(\sigma E(t)+\eta I_A(t)+I(t)\right)-(\lambda+\alpha+\xi)Q_E(t) \tag{18}$$

$$\frac{\mathrm{d}H(t)}{\mathrm{d}t}=\lambda Q_E(t)+\mu_t I(t)-\gamma_3 H(t) \tag{19}$$

$$\frac{\mathrm{d}D(t)}{\mathrm{d}t}=(1-\kappa_t)\gamma_3 H(t) \tag{20}$$

$$\frac{\mathrm{d}R(t)}{\mathrm{d}t}=\gamma_1 I_A(t)+\gamma_2 I(t)+\kappa_t\gamma_3 H(t)-\tau R(t) \tag{21}$$

2.4. Parameter Assignment and Estimation during the High-Intensity Control Period

Given parameters c_0, p, σ, η, ω, λ, δ, κ_m, γ_1, γ_2, and γ_3, the initial infection rate, and the secondary infection rate (as the proportion of uninfected individuals post-close contact isolation) remained relatively unchanged in these two stages.

Therefore, parameters β, τ, α, q_0 and ξ were fitted during the low-intensity control period. The initial values for $Q_S(t_0)=0$, S, E, I_A, I, Q_E, H, D, and R were derived from the final values of each state following the computation of the low-intensity control period model. The disease transmission process in the high-intensity control period can be simulated using equations

(14)-(22). The high-intensity control period model consists of seven parameters: α_1, α_2, α_3, a, b, μ_m, and q_m. Several parameters within the model require fitting. A genetic algorithm was employed to optimize these unknown parameters, utilizing epidemic data from Shanghai for the period of April 16, 2022, to July 1, 2022, as presented in the **Appendix**.

Table 2 shows the fitting results and detailed definitions of each parameter.

Table 2. Phase II model parameter assignment and significance.

Parameter	Definitions	Estimated Mean Value
c_0	The minimum daily contact rate of infected persons	2 [33]
σ	Latent infection rate attenuation factor	0.50
η	Latent infection rate attenuation factor	0.70 [28]
p	Proportion of dominant infection	0.40
ω	The rate of latency to onset	1/5.2 [29]
γ_1	Recovery rate of asymptomatic patients	1/6 [30]
γ_2	Recovery rate of patients	1/8 [31]
γ_3	Recovery rate of diagnosed patients	1/10 [28]
λ	Diagnosis rate of isolated close contacts	1/7 [31]
δ	Isolation susceptible lift rate	1/14
κ_m	The maximum recovery rate of patients diagnosed under current conditions	0.9909
α_1	Exponential attenuation coefficient of contact rate	0.63
α_2	Isolation ratio index increasing coefficient	0.50
α_3	Index increasing coefficient of diagnosis rate	0.02
a	Recovery rate coefficient of confirmed patients	0.90
b	Incremental coefficient of recovery rate index of confirmed patients	0.001
μ_1	Initial diagnosis rate of onset	0.16
μ_m	The fastest rate of diagnosis	0.92
q_m	Maximum isolation ratio	0.90

3. Empirical Analysis

3.1. Model Fitting Effect during the Low-Intensity Control Period

The officially confirmed epidemic data from Shanghai, covering February 22, 2022, to April 15, 2022, were utilized. A genetic algorithm was employed for data fitting, and the effectiveness of the fitting was assessed using the goodness-of-fit metric. Figure 3 shows the process of curve fitting.

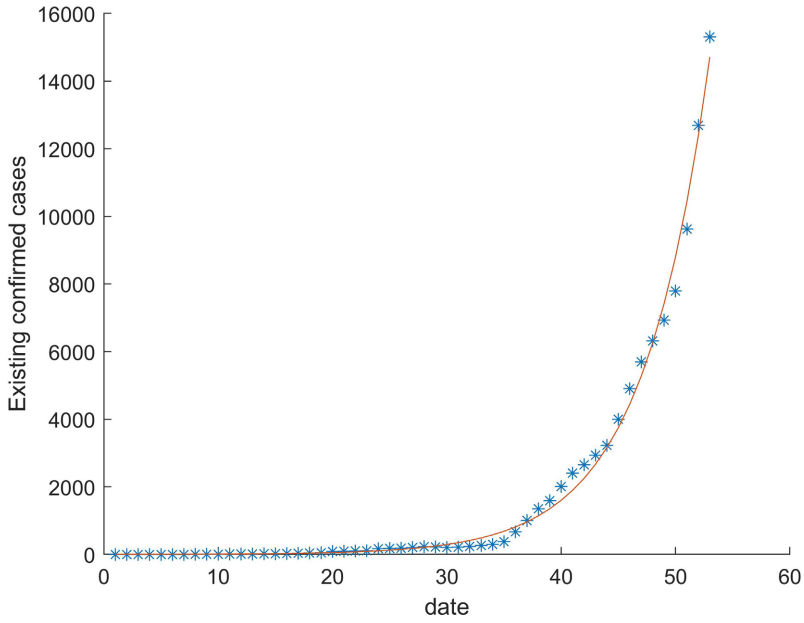

Figure 3. Low-intensity control period model fitting effect diagram.

3.2. Model Fitting Effect during the High-Intensity Control Period

The officially confirmed epidemic data from Shanghai, covering April 15, 2022, to July 1, 2022, were utilized. A genetic algorithm was employed for data fitting, and the effectiveness of the fitting was assessed using the goodness-of-fit metric. **Figure 4** shows the process of curve fitting.

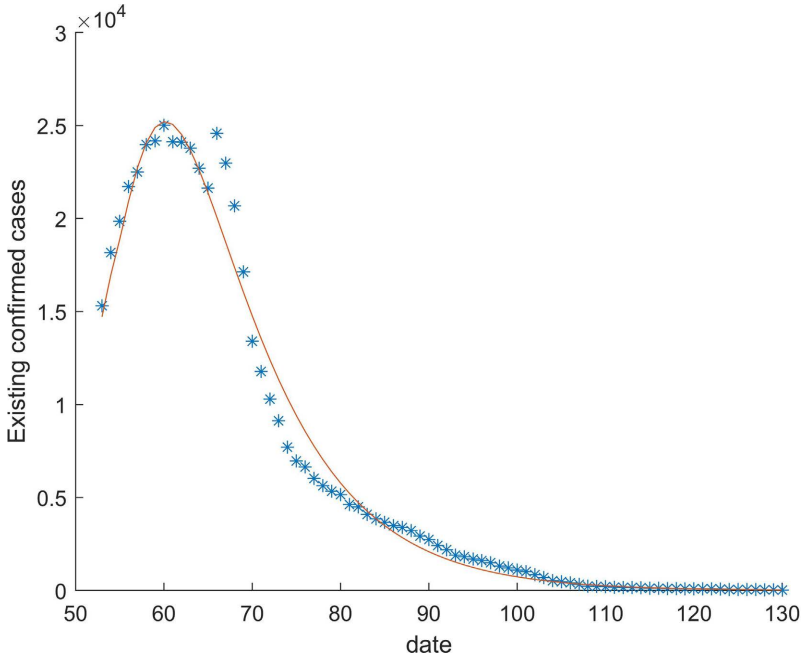

Figure 4. High-intensity control period model fitting effect diagram.

Figure 5 shows the global fitting effect of the two-stage model.

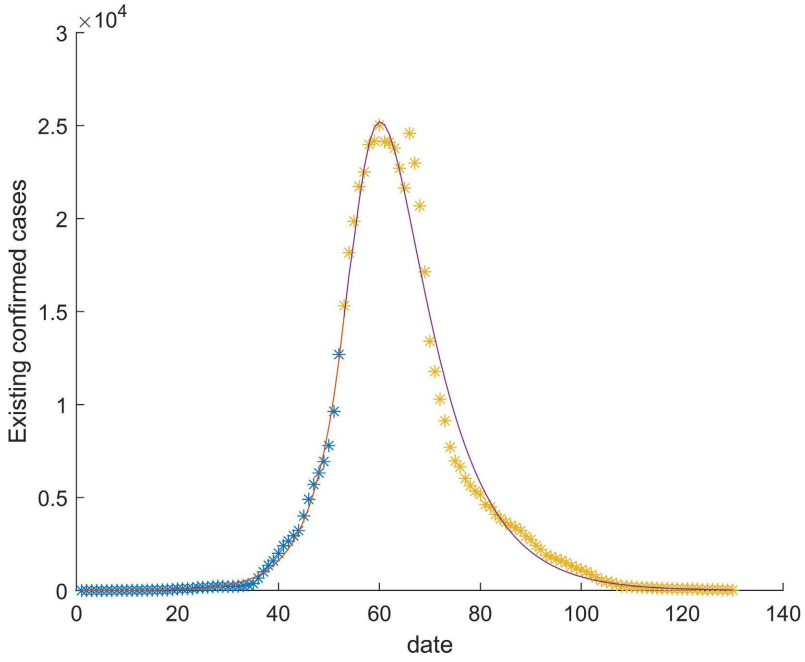

Figure 5. Two-stage model overall fitting effect diagram.

Table 3 shows the R-squared for the first and second stages of the model.

Table 3. The R-squared of two-stage models.

Region	Stage	R-squared
Shanghai	The first stage (53 days)	99.2%
Shanghai	The second stage (78 days)	98.3%

The model's efficacy was assessed by contrasting the discrepancies between the simulated and actual values. During the first stage, spanning 53 days, the model's goodness of fit was determined to be 99.2%, while for the second stage, over a period of 78 days, it exhibited a goodness of fit of 98.3%. This demonstrates the model's remarkable fitting effect, effectively mirroring the trajectory of the epidemic.

3.3. Basic Regeneration Number

As Equations (1)-(7) operate independently of Equation (8), per the mathematical model of the initial stage, only the following subsystems require analysis:

$$\frac{\mathrm{d}S(t)}{\mathrm{d}t} = -c_2\beta\frac{S(t)}{N}\left(\sigma E(t)+\eta I_A(t)+I(t)\right)+\tau R(t)+\alpha Q_E(t) \tag{22}$$

$$\frac{\mathrm{d}E(t)}{\mathrm{d}t} = (1-q_0)c_2\beta\frac{S(t)}{N}\left(\sigma E(t)+\eta I_A(t)+I(t)\right)-\omega E(t) \tag{23}$$

$$\frac{\mathrm{d}I_A(t)}{\mathrm{d}t} = (1-p)\omega E(t)-\gamma_1 I_A(t)+\xi Q_E(t) \tag{24}$$

$$\frac{\mathrm{d}I(t)}{\mathrm{d}t} = p\omega E(t) - (\gamma_2 + \mu_2) I(t) \tag{25}$$

$$\frac{\mathrm{d}Q_E(t)}{\mathrm{d}t} = q_0 c_2 \beta \frac{S(t)}{N} \left(\sigma E(t) + \eta I_A(t) + I(t)\right) - (\lambda + \alpha + \xi) Q_E(t) \tag{26}$$

$$\frac{\mathrm{d}H(t)}{\mathrm{d}t} = \lambda Q_E(t) + \mu_2 I(t) - \gamma_3 H(t) \tag{27}$$

$$\frac{\mathrm{d}R(t)}{\mathrm{d}t} = \gamma_1 I_A(t) + \gamma_2 I(t) + \kappa_0 \gamma_3 H(t) - \tau R(t) \tag{28}$$

At present, the model can be reformulated as follows:

$$\frac{\mathrm{d}x}{\mathrm{d}t} = F(x) - V(x) \tag{29}$$

$$F(x) = \begin{pmatrix} (1-q_0) c_2 \beta \dfrac{S(t)}{N} \left(\sigma E(t) + \eta I_A(t) + I(t)\right) \\ 0 \\ 0 \\ q_0 c_2 \beta \dfrac{S(t)}{N} \left(\sigma E(t) + \eta I_A(t) + I(t)\right) \\ 0 \\ 0 \\ 0 \end{pmatrix} \tag{30}$$

$$V(x) = \begin{pmatrix} \omega E \\ -(1-p)\omega E + \gamma_1 I_A - \xi Q_E \\ -p\omega E + (\gamma_2 + \mu_2) I \\ (\lambda + \alpha + \xi) Q_E \\ -\lambda Q_E - \mu_2 I + \gamma_3 H \\ -\gamma_1 I_A - \gamma_2 I - \kappa_0 \gamma_3 H + \tau R \\ c_2 \beta \dfrac{S(t)}{N} \left(\sigma E(t) + \eta I_A(t) + I(t)\right) - \tau R - \alpha Q_E \end{pmatrix} \tag{31}$$

The expression for the basic reproduction number during the low-intensity control periods can be derived through calculations using the next-generation matrix method.

$$R_1 = 1 + (\kappa_0 - 1) \left(\frac{\lambda q_0}{\alpha + \xi + \lambda} + \frac{\mu_2 p (1 - q_0)}{\gamma_2 + \mu_2} \right) \tag{32}$$

In the high-intensity management and control phase, the Q_S compartment for isolating susceptible individuals is introduced. The reproduction number for the second stage is computed using the same method.

$$R_2 = 1 + \frac{\beta(\kappa_t - 1)}{\beta + q_t - \beta q_t} \left(\frac{p\mu_t}{\gamma_2 + \mu_2} + \frac{\lambda q_t}{\alpha + \xi + \lambda} \right) \tag{33}$$

$R_1 = 0.998$, $R_2 = 0.996$, with these reproduction numbers falling below 1, it signifies that the governmental preventative and control measures have been effective in curtailing the spread of the epidemic.

4. Prediction and Analysis

Despite the high transmissibility of pathogens similar to the novel coronavirus, cases can be effectively managed with appropriate epidemic prevention strategies. To examine the impact of intensified epidemic control measures on the overall trajectory of the epidemic, we selected four discrete temporal nodes for simulation. These simulations aim to scrutinize the effects of intensifying epidemic control measures. The results highlight that by swiftly implementing enhanced epidemic prevention and control measures, the government can significantly reduce the extent of the epidemic. Figure 6 shows the simulation of the spread of the epidemic.

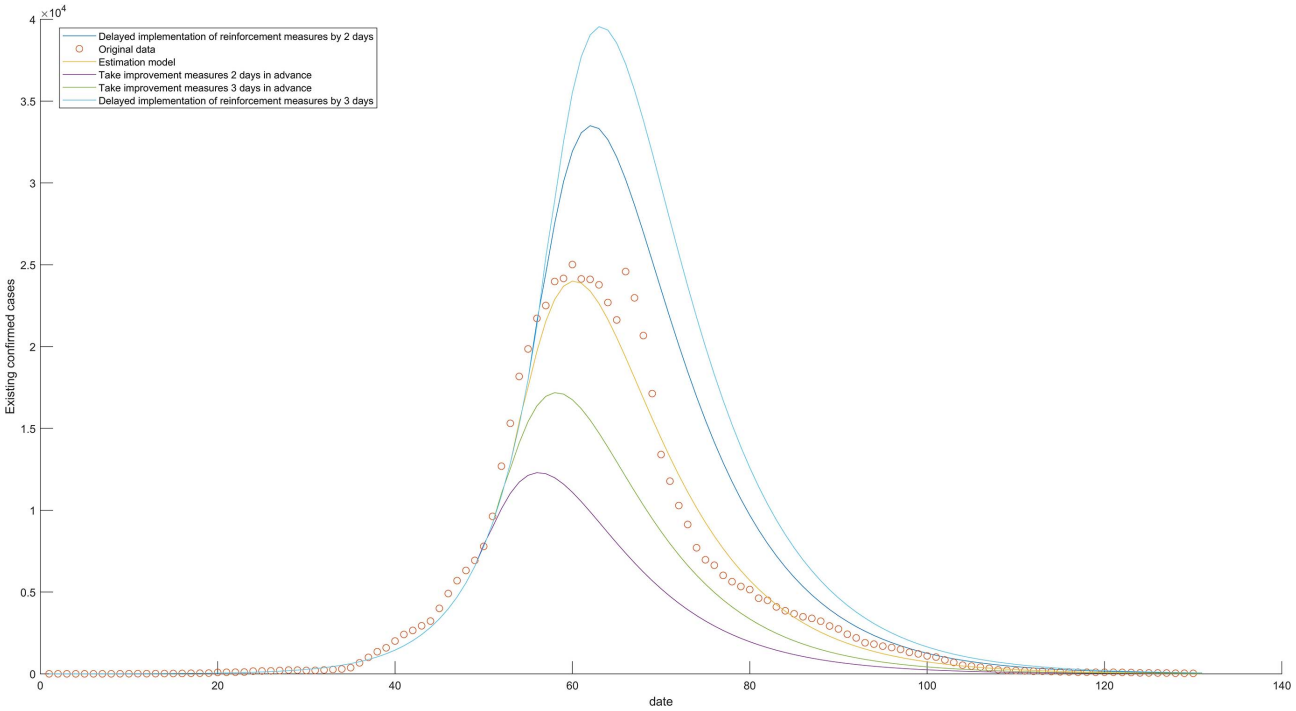

Figure 6. Simulation of the spread of the epidemic.

Based on the above conclusion, we set up four control scenarios for comparison, Table 4 shows the multi-stage control scenarios.

Table 4. Multi-stage control scenarios.

Scene	Control intensity	Key parameter changes
S_1	No control (baseline)	$q_t = 0, c_t = 10, \mu_t = 0.1$
S_2	Low intensity control (actual)	Same as Chapter 5 parameter setting
S_3	Strengthen control 5 days in advance	$R_0 = 0.94$
S_4	Strengthen control by delaying 5 days	$R_0 = 1.2$

Corresponding to the four scenarios $S_1 - S_4$, use formula (34)

$$I_{total} = \int_{t_0}^{t_{end}} \left[pwE(t) + (1-p)wE(t) \mathrm{d}t \right] \tag{34}$$

Calculate the cumulative infection scale of the four scenarios in Table 5. By observing the comparative data of cumulative infection scale at each stage, we can infer that there is a critical threshold for the impact of the timeliness of control on the scale of transmission, and the pathogen appears to exceed the threshold in the early transmission with linear growth characteristics, early management and control can interrupt the positive feedback cycle and avoid the transmission from entering an uncontrollable stage. Its general golden window period is 3 - 5 days.

Table 5. Comparison of the cumulative infection scale at each stage.

Scene	Cumulative number of infected persons (10,000)	Reduction ratio compared with S_1
S_1	632.5	—
S_2	184.2	70.9%
S_3	121.7	80.8%
S_4	257.9	59.2%

In particular, some dynamic parameters in the model reflect the strength of control measures, and the impact of changes in their values on the output of results is also an important evaluation index for evaluating disease control policies. Therefore, we use Sobol sensitivity analysis to quantify the contribution of each control parameter.

$$C_i = \frac{Var(X_i)\left(E_{x_i}(Y \mid x_i)\right)}{Var(Y)} \tag{35}$$

See Table 6 for the calculation results using Equation (35), we can clearly draw such a conclusion: isolation measures are the most critical lever to inhibit transmission, and limiting the population contact rate and improving the speed of admission also have a certain impact on the final results.

Table 6. The contribution degree of each parameter.

Parameter	Contribution degree	Main mechanism of action
q_t	41.2%	Increasing the isolation ratio directly reduces the effective contact rate
C_t	33.7%	Decreasing contact rate reduces the formation probability of propagation chain
μ_t	18.5%	Accelerate the diagnosis and isolation, shorten the infection period
k_t	6.6%	Improve the cure rate and reduce the risk of secondary infection

Although the two-stage model proposed in this study demonstrates high precision in fitting the Shanghai epidemic data, there are several limitations that may

affect the reliability of the results. First, the model parameters are obtained through genetic algorithm fitting, and their accuracy is highly dependent on the completeness and representativeness of the data. If actual parameters exhibit regional, it may lead to predicted results deviating from the true trend. Second, the model assumes that population contact patterns are uniformly distributed and that some individuals possess innate immunity. However, real-world population heterogeneity, the complexity of social networks, and the dynamic changes in immunity may weaken the validity of these assumptions. Future research can enhance the model's adaptability and predictive capabilities by incorporating stochastic processes, stratified population structures, and dynamic feedback mechanisms.

5. Conclusions

In response to the transmission characteristics of highly infectious pathogens, we have refined a two-stage epidemic dynamic model, SEIRHDR_Q. This model incorporates time-varying parameters, such as the recovery rate, and accounts for the comprehensive impact of epidemic prevention and control measures on disease progression, ensuring a close alignment with real-world scenarios. Our analysis indicates that timely enhancements in epidemic control measures can significantly reduce the number of confirmed cases in hospitals, thus alleviating pressure on the medical system.

From the parameter analysis of the developed model, it is evident that during a highly infectious epidemic, heightened public awareness, restrictions on public activities, and other epidemic prevention measures can effectively diminish the epidemic's peak and 202 abbreviate its duration.

Conflicts of Interest

The authors declare no conflicts of interest regarding the publication of this paper.

References

[1] Mwalili, S., Kimathi, M., Ojiambo, V., Gathungu, D. and Mbogo, R. (2020) SEIR Model for COVID-19 Dynamics Incorporating the Environment and Social Distancing. *BMC Research Notes*, **13**, Article No. 352. https://doi.org/10.1186/s13104-020-05192-1

[2] Zhou, T., Liu, Q., Yang, Z., Liao, J., Yang, K., Bai, W., *et al.* (2020) Preliminary Prediction of the Basic Reproduction Number of the Wuhan Novel Coronavirus 2019-nCoV. *Journal of Evidence-Based Medicine*, **13**, 3-7. https://doi.org/10.1111/jebm.12376

[3] Tang, B., Wang, X., Li, Q., Bragazzi, N.L., Tang, S., Xiao, Y., *et al.* (2020) Estimation of the Transmission Risk of 2019-nCoV and Its Implication for Public Health Interventions. *Journal of Clinical Medicine*, **9**, Article 462. https://doi.org/10.3390/jcm9020462

[4] Li, J., Zhong, J., Ji, Y. and Yang, F. (2021) A New SEIAR Model on Small-World Networks to Assess the Intervention Measures in the COVID-19 Pandemics. *Results in*

Physics, **25**, Article 104283. https://doi.org/10.1016/j.rinp.2021.104283

[5] Din, R.U. and Algehyne, E.A. (2021) Mathematical Analysis of COVID-19 by Using SIR Model with Convex Incidence Rate. *Results in Physics*, **23**, Article 103970. https://doi.org/10.1016/j.rinp.2021.103970

[6] Liu, L., Jiang, D. and Hayat, T. (2021) Dynamics of an SIR Epidemic Model with Varying Population Sizes and Regime Switching in a Two Patch Setting. *Physica A*: *Statistical Mechanics and Its Applications*, **574**, Article 125992. https://doi.org/10.1016/j.physa.2021.125992

[7] Alenezi, M.N., Al-Anzi, F.S. and Alabdulrazzaq, H. (2021) Building a Sensible SIR Estimation Model for COVID-19 Outspread in Kuwait. *Alexandria Engineering Journal*, **60**, 3161-3175. https://doi.org/10.1016/j.aej.2021.01.025

[8] De la Sen, M., Alonso-Quesada, S., Ibeas, A. and Nistal, R. (2021) On a Discrete SEIR Epidemic Model with Two-Doses Delayed Feedback Vaccination Control on the Susceptible. *Vaccines*, **9**, Article 398. https://doi.org/10.3390/vaccines9040398

[9] Kundu, S., Jana, D. and Maitra, S. (2021) Study of a Multi-Delayed SEIR Epidemic Model with Immunity Period and Treatment Function in Deterministic and Stochastic Environment. *Differential Equations and Dynamical Systems*, **32**, 221-251. https://doi.org/10.1007/s12591-021-00568-6

[10] Li, Y., Zhang, X. and Cao, H. (2021) Large Time Behavior in a Diffusive SEIR Epidemic Model with General Incidence. *Applied Mathematics Letters*, **120**, Article 107322. https://doi.org/10.1016/j.aml.2021.107322

[11] Youssef, H., Alghamdi, N., Ezzat, M.A., El-Bary, A.A. and Shawky, A.M. (2021) Study on the SEIQR Model and Applying the Epidemiological Rates of COVID-19 Epidemic Spread in Saudi Arabia. *Infectious Disease Modelling*, **6**, 678-692. https://doi.org/10.1016/j.idm.2021.04.005

[12] Ren, Y., Wang, Y., Xia, L., Liu, W. and Tao, R. (2024) Forecasting Hospital Outpatient Volume Using an Optimized Medical Two-Stage Hybrid Grey Model. *Grey Systems*: *Theory and Application*, **14**, 671-707. https://doi.org/10.1108/gs-01-2024-0005

[13] Li, M., Zhang, C., Ding, M. and Lv, R. (2022) A Two-Stage Stochastic Variational Inequality Model for Storage and Dynamic Distribution of Medical Supplies in Epidemic Management. *Applied Mathematical Modelling*, **102**, 35-61. https://doi.org/10.1016/j.apm.2021.09.033

[14] Anderson, R.M. and May, R.M. (1991) Infectious Diseases of Humans. Oxford University Press.

[15] Busenberg, S. and van den Driessche, P. (1990) Analysis of a Disease Transmission Model in a Population with Varying Size. *Journal of Mathematical Biology*, **28**, 257-270. https://doi.org/10.1007/bf00178776

[16] Capasso, V. (1993) Mathematical Structure of Epidemic Systems. Springer. https://doi.org/10.1007/978-3-540-70514-7

[17] Capasso, V. and Serio, G. (1978) A Generalization of the Kermack-Mckendrick Deterministic Epidemic Model. *Mathematical Biosciences*, **42**, 43-61. https://doi.org/10.1016/0025-5564(78)90006-8

[18] Diekmann, O., Heesterbeek, J.A.P. and Metz, J.A.J. (1990) On the Definition and the Computation of the Basic Reproduction Ratio R_0 in Models for Infectious Diseases in Heterogeneous Populations. *Journal of Mathematical Biology*, **28**, 365-382. https://doi.org/10.1007/bf00178324

[19] Evans, N.D. (2001) A Control Theoretic Approach to Containing the Spread of Rabies. *Mathematical Medicine and Biology*, **18**, 1-23.

https://doi.org/10.1093/imammb/18.1.1

[20] Hethcote, H.W. (2000) The Mathematics of Infectious Diseases. *SIAM Review*, **42**, 599-653. https://doi.org/10.1137/s0036144500371907

[21] Holling, C.S. (1965) The Functional Response of Predators to Prey Density and Its Role in Mimicry and Population Regulation. *Memoirs of the Entomological Society of Canada*, **97**, 5-60. https://doi.org/10.4039/entm9745fv

[22] Hsieh, Y. and Sheu, S. (2001) The Effect of Density-Dependent Treatment and Behavior Change on the Dynamics of HIV Transmission. *Journal of Mathematical Biology*, **43**, 69-80. https://doi.org/10.1007/s002850100087

[23] Ivlev, V.S. (1961) Experimental Ecology of the Feeding of Fishes. Yale University Press.

[24] Li, M.Y., Smith, H.L. and Wang, L. (2001) Global Dynamics of an SEIR Epidemic Model with Vertical Transmission. *SIAM Journal on Applied Mathematics*, **62**, 58-69. https://doi.org/10.1137/s0036139999359860

[25] Liu, W., Hethcote, H.W. and Levin, S.A. (1987) Dynamical Behavior of Epidemiological Models with Nonlinear Incidence Rates. *Journal of Mathematical Biology*, **25**, 359-380. https://doi.org/10.1007/bf00277162

[26] Zhang, Y., You, C., Cai, Z., Sun, J., Hu, W. and Zhou, X. (2020) Prediction of the COVID-19 Outbreak in China Based on a New Stochastic Dynamic Model. *Scientific Reports*, **10**, Article No. 21522. https://doi.org/10.1038/s41598-020-76630-0

[27] Ding, Z.X., Song, W.Y., Fang, X.Y., Wang, K., Bao, C.J., Chen, F., *et al.* (2020) Forecasting the Epidemic Trend of Novel Coronavirus Pneumonia in Wuhan, Hubei Province Based on SEIAQR Dynamic Model. *Chinese Journal of Health Statistics*, **37**, 327-330, 334.

[28] Cui, J.A., Lv, J.L., Guo, S.B. and Chen, T.M. (2020) Dynamic Model of Emerging Infectious Diseases—Applied to the Transmission Analysis of COVID-19 in 2019. *Acta Mathematicae Applicatae Sinica*, **43**, 147-155.

[29] Li, Q., *et al.* (2020) Early Transmission Dynamics in Wuhan, China, of Novel Coronavirus Infected Pneumonia. *The New England Journal of Medicine*, **382**, 1199-1207.

[30] Shao, P. and Shan, Y. (2020) Beware of Asymptomatic Transmission: Study on 2019-nCoV Prevention and Control Measures Based on Extended SEIR Model. Preprint. https://doi.org/10.1101/2020.01.28.923169

[31] Tang, B., Wang, X., Li, Q., Bragazzi, N.L., Tang, S., Xiao, Y., *et al.* (2020) Estimation of the Transmission Risk of the 2019-nCoV and Its Implication for Public Health Interventions. *Journal of Clinical Medicine*, **9**, Article 462. https://doi.org/10.3390/jcm9020462

[32] Du, Y.B. (2021) Research on COVID-19 Epidemic Prevention and Control Strategies Based on Infectious Disease Models and Statistical Analysis Methods. PhD Dissertation, Hunan Normal University.

[33] Bai, N., Song, C.W. and Xu, R. (2020) Research on COVID-19 Epidemic Prediction and Control Strategies Based on Dynamic Models. *Acta Mathematicae Applicatae Sinica*, **43**, 483-493.

[34] Shanghai Municipal Health Commission. https://wsjkw.sh.gov.cn/xwzx/#

Appendix

The epidemic data of Shanghai from February 22, 2022 to July 1, 2022 (see Table A1) was provided by the daily data of the Shanghai Municipal Health Commission [34].

Table A1. Data from 22 February to 1 July 2022 (Shanghai).

Data	Cumulative Death	Existing confirmed cases	Data	Cumulative Death	Existing confirmed cases
22 February 2022	0	0	28 April 2022	337	24,584
23 February 2022	0	0	29 April 2022	384	22,979
24 February 2022	0	0	30 April 2022	422	20,674
25 February 2022	0	0	1 May 2022	454	17,127
26 February 2022	0	0	2 May 2022	474	13,400
27 February 2022	0	0	3 May 2022	490	11,775
28 February 2022	0	0	4 May 2022	503	10,284
1 March 2022	0	1	5 May 2022	515	9127
2 March 2022	0	4	6 May 2022	528	7704
3 March 2022	0	6	7 May 2022	536	6970
4 March 2022	0	9	8 May 2022	547	6636
5 March 2022	0	9	9 May 2022	553	6017
6 March 2022	0	12	10 May 2022	560	5631
7 March 2022	0	16	11 May 2022	565	5338
8 March 2022	0	19	12 May 2022	567	5149
9 March 2022	0	23	13 May 2022	568	4621
10 March 2022	0	34	14 May 2022	571	4494
11 March 2022	0	39	15 May 2022	575	4091
12 March 2022	0	45	16 May 2022	576	3852
13 March 2022	0	86	17 May 2022	579	3671
14 March 2022	0	95	18 May 2022	580	3486
15 March 2022	0	100	19 May 2022	580	3390
16 March 2022	0	108	20 May 2022	581	3216
17 March 2022	0	165	21 May 2022	584	2922
18 March 2022	0	173	22 May 2022	585	2741
19 March 2022	0	180	23 May 2022	586	2419
20 March 2022	0	203	24 May 2022	587	2195
21 March 2022	0	226	25 May 2022	588	1898
22 March 2022	0	224	26 May 2022	588	1814
23 March 2022	0	208	27 May 2022	588	1692
24 March 2022	0	211	28 May 2022	588	1607
25 March 2022	0	236	29 May 2022	588	1494

Continued

26 March 2022	0	264	30 May 2022	588	1314
27 March 2022	0	296	31 May 2022	588	1218
28 March 2022	0	375	1 June 2022	588	1095
29 March 2022	0	671	2 Jund 2022	588	1023
30 March 2022	0	1006	3 June 2022	588	848
31 March 2022	0	1352	4 June 2022	588	697
1 April 2022	0	1589	5 June 2022	588	528
2 April 2022	0	2005	6 June 2022	588	472
3 April 2022	0	2406	7 June 2022	588	408
4 April 2022	0	2653	8 June 2022	588	334
5 April 2022	0	2934	9 June 2022	588	237
6 April 2022	0	3224	10 June 2022	588	213
7 April 2022	0	4001	11 June 2022	588	197
8 April 2022	0	4906	12 June 2022	588	180
9 April 2022	0	5695	13 June 2022	588	160
10 April 2022	0	6318	14 June 2022	588	161
11 April 2022	0	6933	15 June 2022	588	142
12 April 2022	0	7788	16 June 2022	588	123
13 April 2022	0	9624	17 June 2022	588	115
14 April 2022	0	12,689	18 June 2022	588	100
15 April 2022	0	15,310	19 June 2022	588	100
16 April 2022	0	18,175	20 June 2022	588	96
17 April 2022	3	19,856	21 June 2022	588	97
18 April 2022	10	21,722	22 June 2022	588	97
19 April 2022	17	22,509	23 June 2022	588	98
20 April 2022	25	23,978	24 June 2022	588	88
21 April 2022	36	24,166	25 June 2022	588	79
22 April 2022	48	25,015	26 June 2022	588	56
23 April 2022	87	24,135	27 June 2022	588	54
24 April 2022	138	24,107	28 June 2022	588	50
25 April 2022	190	23,775	29 June 2022	588	48
26 April 2022	238	22,694	30 June 2022	588	36
27 April 2022	285	21,629	1 July 2022	588	34